Final Draft
of the original manuscript:

Dogan, B.; Nikbin, K.; Petrovski, B.; Ceyhan, U.; Dean, D.W.:
Code of practice for high-temperature testing of weldments
In: International Journal of Pressure Vessels and Piping (2006) Elsevier

DOI: 10.1016/j.ijpvp.2006.08.011

Code of Practice for High Temperature Testing of Weldments

B.Dogan[1*], K.Nikbin[2], B.Petrovski[1], U.Ceyhan[1] and D.W.Dean[3]

[1] GKSS Research Center, Max-Planck-Str.1 D-21502 Geesthacht, Germany.
[2] Imperial College, Exhibition Road, London, SW7 2AZ, UK.
[3] British Energy Generation Ltd., Barnwood, Gloucester, GL4 3RS, UK.

ABSTRACT: The present paper reports on a Code of Practice (CoP) for high temperature testing of weldments for industrially relevant specimens. Novel aspects of the CoP include advice for testing weldment zones using different specimen geometries. Those specimens differ from the standard Compact Tension (CT) specimen proposed in the only available creep crack growth testing standard ASTM E1457. Recommendations for the required number of tests, techniques for testing, treatment of test records, reduction of test data and data analysis are presented. Associated specimen selection guidelines for industrial creep crack initiation and growth testing are also described. Validation tests carried out on P22 and P91 weldments and base metals of 316H steel and C-Mn steel using relevant specimen geometries are briefly described. The CoP contains recommended K and C* solutions, Y functions and η factors, which are used to determine values of the fracture parameters K and C^* for the specimen geometries considered. Information from these new tests, together with a review of previous creep crack growth tests on non-standard geometries, have been used in recommending the best method of analysis for creep crack initiation and creep crack growth data for a range of creep brittle to creep ductile welded materials.

KEYWORDS: Code of Practice, Fracture mechanics, Weldments, Creep crack initiation, Creep crack growth, C^*, Specimen geometry, η factor.

Nomenclature

a	Crack length
a_o, a_f	Initial and final crack length measurements
Δa	Amount of crack growth
$\dot{a}$, da/dt	Crack growth rate
B, B_n, B_e	Specimen thickness, net specimen thickness, effective specimen thickness
CCG, CCI	Creep Crack Growth, Creep Crack Initiation
CMOD	Crack Mouth Opening Displacement
C_o	Compliance at time zero
CoP	Code of Practice
C(T)	Compact Tension Specimen
CRETE	EC Project CRETE (Ref.2)
CS(T)	C-Shape Specimen in Tension
C_t	Crack tip parameter for transient to extensive creep
C^*	Steady state creep fracture mechanics parameter
$C^*(t)$	Experimentally determined value of C^* at test time, t
DEN(T)	Double Edge Notch Tensile Specimen
D', D'_i	Material constant in $\dot{a}$ correlations with K
D_o ,D_i	Material constant in $\dot{a}$ correlations with C^*
EDM	Electrical Discharge Machined
ESIS	European Structural Integrity Society
E	Elastic modulus
E'	Effective elastic modulus for plane strain

* Corresponding author.
E-mail address: bilal.dogan@gkss.de (Bilal Dogan)

FS	Fracture surface
HAZ	Heat Affected Zone
H	Specimen Height
H^{LLD}	Geometric function to calculate C^* from load line displacement rate
H^{CMOD}	Geometric function to calculate C^* from crack mouth opening displacement rate
J	J-integral crack tip parameter
K, K_n	Stress intensity factor, Stress intensity factor for net section thickness
K^c_{mat}	Creep crack initiation toughness
L	Half span length
LLD	Load Line Displacement
LVDT	Linear Variable Displacement Transducer
M	Bending moment
m'	Material constant in $\dot{a}$ correlations with K
M(T)	Middle Crack Tension specimen
N	Stress exponent in power-law plasticity
n	Power-law creep stress exponent
P	Applied load
PD	Potential Drop
R_i	Inner radius of CS(T) specimen
R_0	Outer radius of CS(T) specimen
SEN(B)	Single Edge Notch Specimen in Bending
SEN(T)	Single Edge Notch Specimen in Tension
TC	Technical Committee
t_i	Time for crack initiation (at Δa=0.2 mm and 0.5 mm)
t_T	Transition time from primary to steady-state creep
U	Area under load-displacement curve
V_i	Value of the potential drop (PD) measurement at initiation
V_0, V_f	Initial and final values of the potential drop (PD) measurement
W	Specimen width or half width
$Y(a/W)$	Geometry factor to calculate K
$\dot{\Delta}_c$	Creep component of load line displacement rate
Δ^{LLD}, $\dot{\Delta}^{LLD}$	Load line displacement, load line displacement rate
$\dot{\Delta}_c^{LLD}$	Component of the load line displacement rate directly associated with the accumulation of creep strains
$\dot{\Delta}_i^{LLD}$	Component of the load line displacement rate directly associated with instantaneous (elastic and plastic) strains
$\dot{\Delta}_{i,e}^{LLD}$	Component of the load line displacement rate directly associated with instantaneous elastic strains
Δ^{CMOD}, $\dot{\Delta}^{CMOD}$	Crack mouth opening displacement, crack mouth opening displacement rate
ε_f^c	Creep ductility
$\dot{\varepsilon}^c$	Creep strain rate
η^{CMOD}	Geometric factor to calculate C^* from crack mouth opening displacement rate
η^{LLD}	Geometric factor to calculate C* from load line displacement rate
ϕ	Material constant in $\dot{a}$ correlations with C^*
λ	Non-dimensional crack velocity
σ	Stress
σ_b	Nominal bending stress
σ_m	Membrane stress

σ_{ref}	Reference stress
v	Poisson's ratio

1. Introduction

The available codes for high temperature crack growth testing and characterization of materials are limited in scope and international acceptance. The most widely used standard for creep crack growth testing of metallic materials [1] mainly addresses testing homogeneous materials in compact tension, C(T), type specimens. Therefore, the outstanding need for high temperature characterization of weldments creep crack initiation and growth in alternative industrial specimens has been the subject of collaborative efforts of ESIS TC11 and the European project CRETE [2], which had the objective of harmonizing testing procedures for these specimens in order to obtain data for use in defect tolerance assessment of components. Recent reviews of high temperature defect assessment procedures [3] and the significance of creep in defect assessment procedures for low to high temperature [4] emphasize the need for reliable creep crack growth data. The British Standard document BS7910 [5] contains some indicative data for creep crack growth assessment, whereas the R5 [6] procedure does not explicitly supply creep crack growth data, except where specifically used to validate the procedures. The present paper outlines the guidelines of a Code of Practice (CoP) for experimental determination and analysis of Creep Crack Initiation (CCI) and Creep Crack Growth (CCG) rate data of weldments including Base Metal (BM), Heat Affected Zone (HAZ) and Weld Metals (WM). CCI is defined as the extension of a pre-existing defect by a small amount of growth, typically 0.2 mm or 0.5 mm. Novel aspects of the CoP include interpretation of potential drop (PD) records, crack size determination and measurement on tested specimen surfaces, crack tip parameter (K, C^*) solutions, $Y(a/W)$ functions and η factors for six specimen types. Validation tests were carried out on P22, P91 Steel weldments, and base materials of Type 316H steel and a C-Mn steel using relevant specimen geometries. Selected results on P22 weldments are presented.

2. CoP for High Temperature Testing of Weldments

2.1. Scope and Use

The present CoP aims to provide recommendations and guidance for a harmonized procedure for measuring and analyzing CCI and CCG characteristics of metallic welded materials using a wide range of industrial fracture mechanics specimen geometries. It will allow laboratories with limited test material to carry out tests on different specimen geometries [7] machined out of various zones of weldments.

2.2. Specimens

The emphasis in the presented CoP is placed on the inclusion of component-relevant industrial specimen geometries [7] made of welded materials. It covers testing and analysis of CCI and CCG in metallic materials at elevated temperature using six different cracked geometries (Fig. 1), for which validation tests have been conducted [2]. Positions of PD and current (I) leads, which are used for crack length monitoring, are shown for each specimen geometry in Fig. 1.

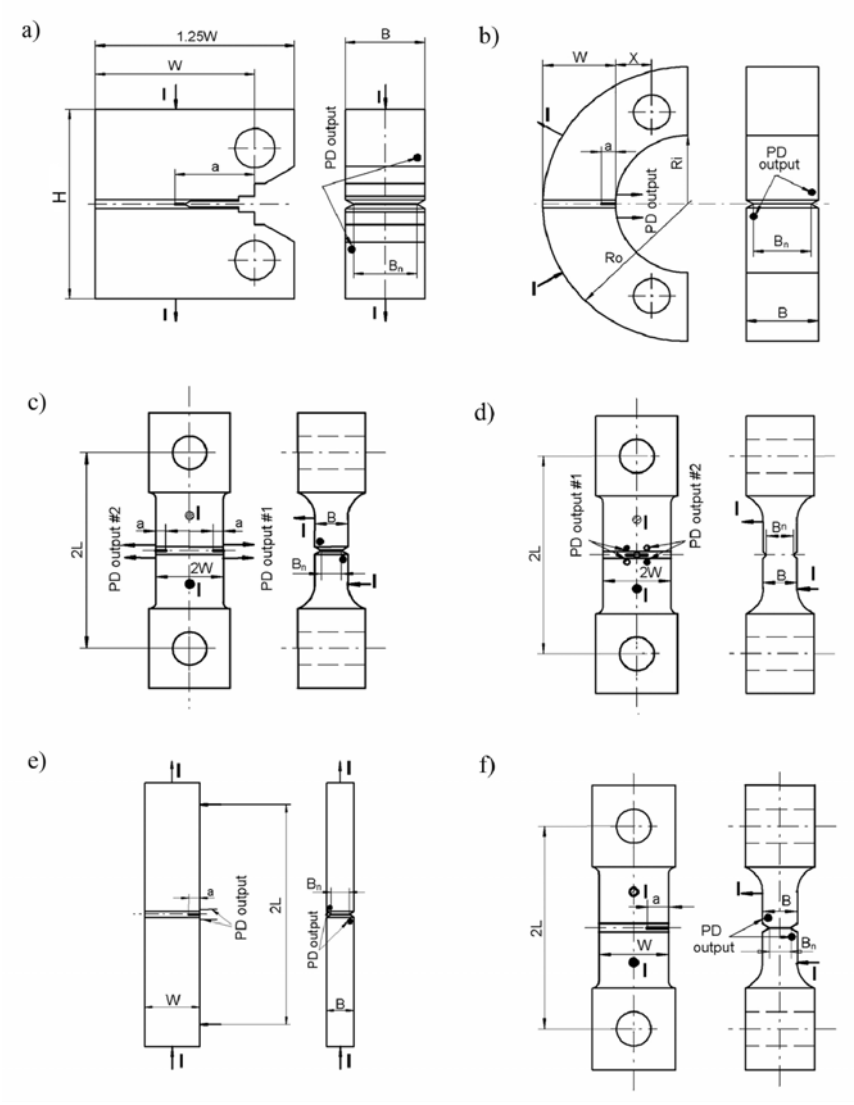

Fig. 1 Specimen geometries a) Compact Tension, C(T); b) C-Shape Tension, CS(T) c) Double Edge Notched Tension, DEN(T); d) Middle cracked Tension, M(T); e) Single Edge Notched Bend, SEN(B); f) Single Edge Notched Tension SEN(T) [2, 7].

Specimen abbreviations and loading arrangements are: Compact Tension C(T), C-Shape Tension CS(T), Double Edge Notched Tension DEN(T), Middle Crack Tension M(T), Single Edge Notched Tension SEN(T), in pin loading, and Single Edge Notched Bend, SEN(B), in three point bending.

2.3. Specimen Geometries

The specimen types shown in Fig. 1, which have been used for experimental and numerical validation are given in Table 1. These specimen sizes and dimensions were chosen to permit validation tests to be conducted on welded steels within the machine capacity available in laboratories. The CoP also permits geometrically similar specimens with different in-plane dimensions to be used and the thickness to width (B/W) ratio can also differ from the values given in Table 1, if required. The initial crack lengths used in the validation tests were

with a_o/W ratio within a range of (0.2-0.4) for DEN(T), M(T) and SEN(T) specimens and (0.3-0.5) for the other specimens.

Table 1. Test specimen geometries [2, 7]

Specimen	Geometry	W (mm)	H, L, R_0 (mm)	B (mm)
C(T)	Compact Tension	50	H=60	25
CS(T)	C-Shape Tension	25	R_0=50	25
DEN(T)	Double Edge Notched Tension	12.5	L=37.5	12.5
M(T)	Middle Tension	12.5	L=37.5	12.5
SEN(B)	Single Edged Notched Bending	25	L=50	12.5
SEN(T)	Single Edge Notched Tension	25	L=37.5	12.5

In Table 1, H is the height of C(T), R_0 is the outer radius of CS(T), and L is the half span of the SEN(B) specimen and the half length (between loading points) of SEN(T), DEN(T) and M(T) specimens.

2.4. Specimen Selection Criteria

This section outlines the main factors, which need to be considered in this process and summarizes the strengths and weaknesses of the standard C(T) specimen and the alternative industrial specimens. Attention is given to the selection of the appropriate specimen geometry for the particular application being considered.

Material availability: The choice of specimen size and geometry depends on the material availability for testing. In many cases, the volume and dimensions of available welded material is limited. This issue is of particular concern when testing material obtained from welded components in both virgin and service exposed conditions. The shape of the material components available can also influence the choice of specimen. The CS(T) specimen is particularly suited to testing material from tubular components and the SEN(T) would be appropriate for blade type components.

Specimen orientation: Components may contain microstructural variations such as in weldments and even micro-voids. Therefore, the orientation of the crack in the specimen should be chosen to be normal to the defect orientation and weaken zone, which might exist in the component being assessed. In addition the tensile and creep material properties in the direction of the orientation chosen as well as various weldment zones should be available as they will be needed for the analysis of the CCI and CCG data. The required specimen orientation, together with the volume and dimensions of available material can significantly influence the choice of specimen geometry.

There are combinations of parent/weld/and HAZ properties that need to be considered in a weldment specimen. Usually for parent and weld properties homogenous specimens cut from these regions can serve the purpose for deriving CCI and CCG properties of these regions. However for HAZ properties which is sandwiched between the parent and the weld material, the specimen has to be designed to align, as best as possible, the line of the HAZ on the crack path. Fig. 2 a) and b) below show the comparison for the a C(T) specimen with weld and the standard specimen containing one material property.

It should be noted that regardless of where the crack path is positioned the crack may grow through a preferred path of least resistance. The reasons for any deviation from the crack plane are discussed and recommendations are made in the CoP as to what the user should do when this occurs.

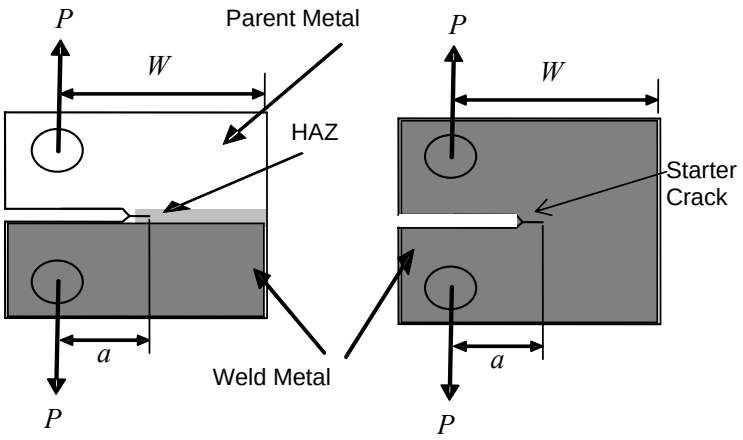

(a) (b)

Fig. 2 Schematic of C(T) specimens indicating the position of the starter crack and of the a) HAZ, b) all weld or base material regions.

Machine capacity: The machine capacity available for performing the creep crack growth tests will have a significant influence on the specimen geometry and dimensions which can be tested for a given material condition. The higher constrained C(T), SEN(B) and CS(T) specimens will require lower test loads for given dimensions, B_n, (W-a), than the DENT(T) and M(T) and SEN(T) geometries.

Component geometry and loading: High temperature crack initiation and growth data are required for assessment of component behaviour in service. It is important to be able to demonstrate that the creep crack growth data obtained are: i) appropriate to the geometry and loading being considered, ii) conservative for the geometry and loading being considered.

In the former case, if service loads are exclusively tensile, the DEN(T) or M(T) specimens may be most appropriate. However, if conservative creep crack growth data are required for a range of applications, it is more appropriate to test highly constrained geometries such as the C(T) or SEN(B).

Specimen thickness: The specimen thickness should normally be chosen to be equal to, or exceed, the section thickness of the component being assessed. Table 1 gives the range of thicknesses that have been validated within European collaborative programmes [2]. However this does not exclude the testing of other thicknesses as long as the tests are checked for validity.

Suitability for crack initiation and crack growth testing: A fatigue pre-crack may be introduced as an initial defect as it is expected that a sharper fatigue crack as compared with EDM may reduce the time for initiation. This is of particular importance for creep crack initiation data. However, this may influence the choice of specimen geometry. Planar specimens with single defects (e.g. C(T), CS(T), SEN(B), SEN(T)) are preferred as difficulties can arise with other types of specimen, e.g. DEN(T) and M(T) specimens which contain two crack tips. Planar specimens with single defects are also preferable for creep crack growth rate determination as non-symmetrical creep crack growth is likely to occur from the two starter crack tips in DEN(T) and M(T) specimens.

3. Strengths and Weaknesses of selected Specimen Geometries

The strength and weaknesses of selected specimen geometries are presented below. The C(T) is the mostly used geometry that serves as a common base for fracture studies, on which the other geometries built. The benefits of using other geometries, which are seen in simulating loading conditions of materials in service are also listed below.

3.1. Standard Compact Tension (C(T)) Specimen Geometry

Strengths

- Highly constrained (for deep cracks, $a/W>0.45$); can be used to generate conservative creep crack initiation and growth data for a range of applications.
- Low load capacity requirement (for a given ligament size).
- Compact; maximum/minimum dimension ratio is low (~2.5).
- Simple pin loading.
- Easy to fatigue pre-crack.
- Suitable for both creep crack initiation and growth testing.
- Best η factors and C^* estimates based on load-line displacements (for deep cracks, $a/W>0.45$).

Field Code Changed

Weaknesses

- Cannot be used for shallow cracks (small a/W) as deformation spreads to the loading pins.
- Could produce rapid fracture in creep-brittle specimens.

3.2. Other Specimen Geometries (CS(T), DEN(T), M(T), SEN(B), SEN(T))

Strengths

- Highly constrained for deeper cracks; can be used to generate conservative creep crack initiation and growth data for a range of applications (CS(T), SEN(B)).
- Low constraint (for low values of a/W); can be used to generate creep crack initiation and growth data for low constraint applications involving tensile loading (DEN(T), M(T), SEN(T)).
- Low load capacity requirement (for a given ligament size) (CS(T), SEN(B)).
- Relatively compact; maximum/minimum dimension ratio is relatively low (4) (CS(T)).
- Particularly suited to testing tubular components (CS(T)).
- Simple pin or thread loading (CS(T)), DEN(T), M(T), SEN(T).
- Easy to fatigue pre-crack (CS(T), SEN(B), SEN(T)).
- Suitable for both creep crack initiation and growth testing (CS(T), M(T), SEN(B), SEN(T)).

Weaknesses

- Large specimen for a given area of defective section (CS(T)).

- Best η factors and C^* estimates require measurements of crack mouth opening rather than load-line displacements (CS(T), DEN(T), M(T), SEN(B), SEN(T))
- Requires a special loading fixture (SEN(B)).
- Constraint can become high for very deep cracks (DEN(T), SEN(T)).
- Maximum/minimum dimension ratio is high (~8) (DEN(T), M(T), SEN(T)).
- High load capacity requirement (for a given ligament size) (DEN(T), M(T), SEN(T)).
- Fatigue pre-cracking can be problematic (due to asymmetry in the two cracks) (DEN(T), M(T)).

4. Specimen Preparation

Specimen preparation consists of spot welding of or screw tightened thermocouples and potential drop (PD) wires, introduction of a sharp starter crack and side-grooving. For positioning of the wires advice should be sought from the PD equipment manufacturer. Current input wires should be placed remote from the crack tip and the potential output wires should be placed on the opposite face of the specimen, aligned near the crack tip, as shown on the specimens in Fig. 1. It is preferable to weld the current input leads to the specimen as this ensures good electrical contact, which is maintained throughout the test.

4.1. Starter Crack

Fatigue pre-cracking is recommended for introducing a starter crack if a flat and straight crack front can be maintained where this may be difficult for weld materials with variations in grain size and hardness. However, an electro-discharge machined (EDM) slit can also be used as a starter crack provided the crack tip radius is 0.05 mm or less [8]. The EDM method is particularly suitable for starter cracks in HAZ and fusion line tests. However, if CCI information is required, fatigue pre-cracking should be used to introduce the starter crack unless it can be demonstrated that equivalent initiation behaviour is obtained using an EDM slit [8,9].

4.2. Side-grooving

Specimen side-grooving (SG), 20% in total, 10% on each side, is generally required to obtain a straight crack front. However, for creep ductile materials, such as the C-Mn steel a total side-groove reduction of up to 40% may be required to produce a straight crack front [2, 10].

5. Tests and Measurement Techniques

The type of testing and measurement equipment is left to the discretion of the users. The restrictions placed on the users are the limits of accuracies with respect to specimen dimensions, temperature, load, displacement, and crack length measurements. Test techniques together with accuracy limits for measuring test variables will provide correct and repeatable test data that help to reduce data scatter. The limits proposed are the same as those used in ASTM E1457 [1]. The Round Robin [2] work focused on constant load tests to determine CCI and CCG behaviour. However, similar techniques can also be used to perform fixed displacement and fixed displacement rate tests. In some cases where the material is very creep brittle stress sensitive, or the industrial operational loading conditions are displacement controlled, it may be advisable to perform constant displacement or constant displacement rate tests. It is recommended, where possible, to compare data from these alternative types of test with those from constant load tests on C(T) specimens.

Significant material inhomogenity exists in single crystals, directionally solidified materials and weldments (including cross-welds and Heat Affected Zone (HAZ) tests). The testing techniques applied to weldments follow the validation carried out on homogeneous

materials [10]. The energy method for deriving the experimental C^* parameter inherently takes into account such inhomogeneities as the creep displacement rate measured is dependent on the type of material that is deforming local to the crack tip.

5.1. Environment

Aggressive environments at high temperatures can significantly affect the CCI and CCG behaviour. Attention must, therefore, be given to the proper selection and control of temperature and environment in data generation. All relevant information should be fully logged for each test in order to identify deviations from the norm as specified in the CoP [7]. Tests are mostly carried out in laboratory air at test temperatures. Tests can also be carried out in vacuum or aggressive atmospheres in order to simulate the service conditions of the structural component to be assessed. Note that aggressive environments can enhance damage and hence affects the crack initiation and growth processes. Nevertheless, providing that creep is the dominant damage mechanism, the methods described here can be used although caution should be exercised in using the data to predict creep crack growth behaviour for other environmental conditions.

5.2. Measurements During Tests

The measured load, potential drop and displacement data are required to be logged starting from the pre-load which is approximately 10 percent of the full load all the way to the end of the test. This information is important for the subsequent analysis of the data using C^* and K particularly for CCI assessment. Any instantaneous deviation from the elastic loading condition prior to creep at or near zero time should be noted. In addition the load/displacement measurements give the specimen's elastic compliance for the initial crack length. The initial elastic displacement at full load and the final elastic displacement during the final unloading should be measured and logged. It is also possible to perform partial unloadings during the test of up to 15 percent of the test load, as a means of monitoring crack size development or if there is concern regarding premature failure of the specimen.

5.3. Crack length measurements

Measuring equipment capable of reliably resolving crack extensions of at least ±0.1 mm at the test temperature is recommended for crack size monitoring. The selected measurement technique must be capable of measuring the average crack size across the thickness. Since crack extension across the thickness of the specimen is not always uniform, surface crack length measurements by optical means are not considered to provide reliable crack size estimates.

Partial unloading compliance may also be used for crack length estimation during the testing although the most commonly used method for crack length monitoring is the potential drop (PD) technique method using either direct current (DC) or alternating current (AC). The methods used are described in detail below.

5.4. Partial-Unloading Compliance

The measurement of compliance from load vs. load line displacement (LLD) data requires loading and unloading, ΔP, of a specimen at time t=0. The expression below is used for time zero compliance,

$$C_0 = \Delta^{LLD} / \Delta P \tag{1}$$

The initial crack length is calculated from the initial compliance at t=0, using formulae relating the crack size to the specimen compliance. The formula is supplied in the literature [11] only for a fatigue pre-cracked C(T) specimen;

$$a_o/W = 1{,}000196 - 4{,}06319\,U_{xo} + 11{,}242\,U_{xo}^2 - 106{,}043\,U_{xo}^3 + 464{,}335\,U_{xo}^4 - 650{,}677\,U_{xo}^5 \quad (2)$$

where $U_{xo}=1/[(B_eE'C_o)^{1/2}+1]$, effective thickness $B_e=B-[(B-B_n)^2/B]$, and $E'=E/(1-\nu^2)$ for plane strain and $E' = E$ for plane stress conditions.

There is a significant influence of elastic modulus, E, on crack length calculation accuracy and it is therefore important to have a reliable value of E obtained at the test temperature. For E values ranging between 100 and 200 GPa the difference in predicted Δa for a C(T) specimen is depicted in Fig.3, which shows that total errors of ± 12 percent can be introduced.

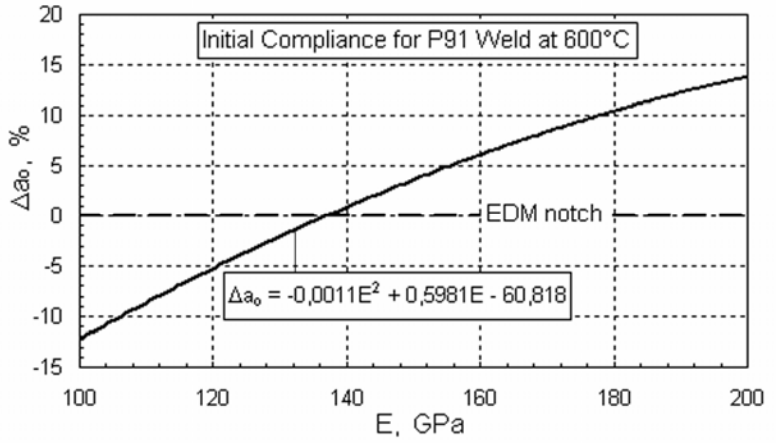

Fig. 3 Variation of crack length Δa_o for a C(T) specimen determined by partial unloading compliance method with elastic modulus E of the material at test temperature.

5.5. Potential Drop Method

Direct current potential drop (DCPD) and alternating current potential drop (ACPD) methods are often applied to monitor crack initiation and growth during testing. The crack size is determined from DCPD data using Johnson's formula given for the C(T) geometry [1]. Correct use of PD data is particularly important when determining CCI as several possible types of PD-time behaviour may be observed as shown schematically in Fig. 4.

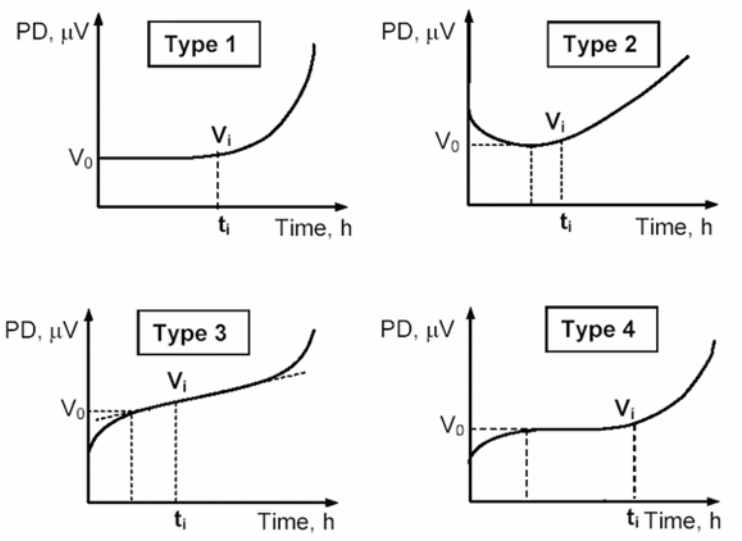

Fig. 4. Types of potential drop (PD) vs. time records in creep crack growth tests

The scatter in crack size using the PD method is increased by the crack channeling with unbroken ligaments as observed on fracture surfaces. An accurate measurement of the initial (a_o) and final (a_f) crack size should be made when the specimen has been broken open outside the furnace after testing. The final measured crack length may be used to calibrate the crack lengths from potential data using Johnson's formula. Alternatively, linear interpolation between measured initial and final crack sizes determined on the broken specimen fracture surface (FS) may be used for crack length calculations.

The comparison of these methods is summarized in Fig. 5 which shows amounts of crack growth determined using DCPD, the compliance method and those from corrected data using a_f from (FS). Excellent agreement is demonstrated between crack length determined from partial unloading compliance and the FS corrected PD method for P91 HAZ material at 600°C.

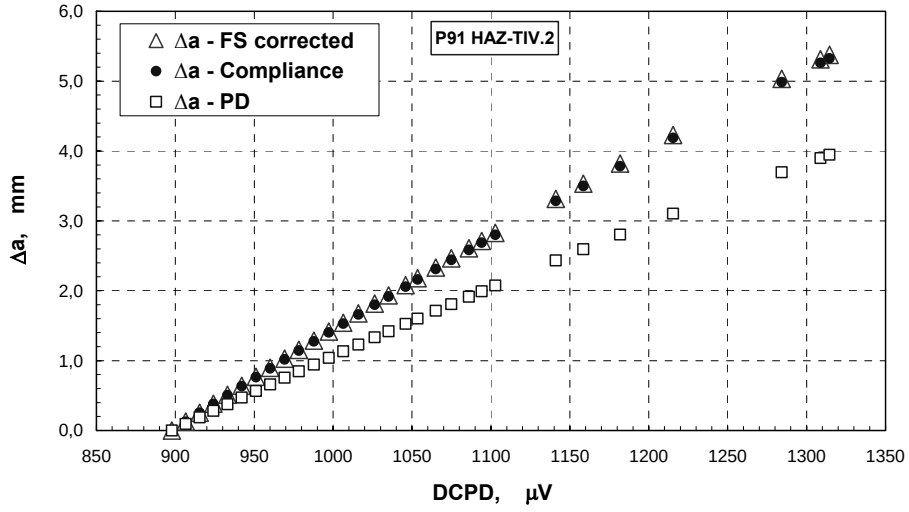

Fig. 5. Δa vs. DCPD, compliance and DCPD with FS correction

From the complete data set, a sufficient number of data points (typically 30–50) are selected to describe the shape of the crack length, and Δ^{LLD} and Δ^{CMOD} vs. time curves. When raw data are sparse or missing, interpolation should be performed without changing the trends in the overall data. In some cases, PD readings decrease after initial loading (which indicates an apparent decrease in the crack length), reach a minimum value and then start to increase (Type 2 in Fig. 4). For such cases, the value of V for all points of decreasing PD output should be taken to be the minimum value before the PD output again started to increase. The initial increase as seen in Type 3 & 4 in Fig.4, recorded prior to crack tip opening is probably due to contacting pre-cracked faces and contacting debris. Therefore, it should not be accounted as the indication of CCG. Any jumps that occur in the PD or LVDT readings without an obvious explanation should be corrected by subtracting the magnitude of the jump in the LVDT or PD reading from the subsequent data points.

5.6. Test Interruption and Termination

Data logging and taking additional readings at the beginning of the test when rapid changes occur is important particularly for CCI studies. Also, when the test nears its final stage and CCG begins to accelerate additional readings should be taken. A decision must be made at some point to stop the test when CCG begins to accelerate towards rupture. It is ideal to stop the test just before failure or when the specimen has reached approximately 90-95% of life. Alternatively, the test should be stopped as soon as both the potential drop and the displacement measurements show an acceleration in crack growth rates and displacement rates, indicating that final failure of the specimen is imminent. On-line crack length calculations using Johnson's formula [1] or unloading compliance measurements as described above may give guidance in deciding when to terminate the test.

5.7. Post Test Measurements and Metallographic Examination

An accurate measure of the initial (a_o) and final (a_f) crack front and crack size should be made when the specimen is broken open outside the furnace after testing. The total crack extension, Δa_f, is derived by subtracting the initial crack size, a_o from the value of the final crack size, a_f. The final crack size shall be determined from fracture surface measurements where possible. The initial and final measured crack lengths are used to compute the incremental crack length from PD measurements obtained during the tests. Post-test measurements are recommended to be carried out on the tested specimens. Any dimensional changes, necking, crack front shape and fracture surface observations should be recorded. Detailed metallography to observe damage ahead of the crack tip, especially when crack initiation is of interest should be performed. Crack tip damage development is examined on completion of the test, on the sectioned half of the specimen, normal to the crack plane, using EDM the other half is broken open by a combination of fatigue and saw cutting, to reveal the fracture surface produced by creep crack growth [12]. If there is failure to stop the test before making the measurements the observations should make use of oxide surface markings using fractography to identify the crack tip profile. The crack size is measured on half of the specimen at a minimum of 8 (or 16 for the full specimen) equally spaced points centred on the specimen mid-thickness line and extending to 0.005W from the roots of the side-groove. The crack size used is the average between the measured lengths. If the ratio due to crack tip bowing between the crack tip centre and the surface exceeds 20 percent, the longer final crack length a_f should be recorded. The measuring instrument shall have an accuracy of 0.025 mm. Alternatively, the fracture surfaces can be recorded using a digital imaging system and downloaded to provide a permanent electronic record. Measurements of mean values of a_o

Field Code Changed

and a_f can then be made from the recorded data using an image analysis computer program based on crack area measurements.

5.8. Determination of displacement rates and CCG rates

The crack length, load-line deflection and time data need to be processed for determining the load-line displacement rate, dΔ/dt, and the creep crack growth rate, da/dt. The data points are chosen consisting of crack length and the corresponding load-line displacement and time such that crack extension between successive data points is of the order of 0.005W. If the crack growth is small, smaller Δa values should be chosen such that a minimum of ten data points will be determined for the total crack growth range.

Both the secant method and the incremental polynomial method can be used in determining the load-line displacement rate, dΔ/dt, and the creep crack growth rate, da/dt [1]. Although the incremental polynomial method smoothes the data, reducing the scatter in rates, for the tests with small crack growth as in small size specimens of weldments, which have usually small number of data points, the secant method is recommended for determining rates. It is also possible to fit alternative mathematical functions relating the load-line displacement and crack growth to time; these functions can then be differentiated to determine load-line displacement and creep crack growth rates. Different fitting functions may yield small difference in crack growth rate data only in CCI. Furthermore, the polynomial method may lead to artificial kinks in fitted data at junction points of different functions.

6. Treatment of Creep Crack Growth

6.1. Creep Crack Growth (CCG) Rate Correlations

The crack tip parameters K or C^* are conventionally used for correlating CCG rate data. However, other crack tip parameters, C_t [13], Q* [14] and local CTOD rate [15] may also be used to correlate CCI and CCG data. Background information on the rationale for employing the fracture mechanics approach in the analysis of creep crack growth data is presented in [7]. In order to correlate da/dt with K or C^*, the required material properties may be obtained from uniaxial and CCG tests. The test conditions, in which the tests are performed, and the data reduction method and fitting may have a considerable influence on the test results. The da/dt values are determined from crack size data using a secant method or seven-point polynomial fit of crack length data. The da/dt vs. time and da/dt vs. C^* correlations may contain kinks due to high degree polynomial fits of crack length or load line deflection that may be misinterpreted as material phenomena such as pop-in in crack growth. Therefore, a low degree of polynomial method of test data is recommended for data fitting procedures. The appropriate solutions for K and C^* are presented for crack growth rate correlations in an annex of [7]. These are valid for the size and specification of the test geometries given in Fig.1. As recommended in the CoP the applied load on a side grooved specimen will be acting over a shorter crack front, equal to the net section thickness B_n, and, therefore, the stress intensity factor will be higher by the following amount [7]:

$$K_n = K\left(\frac{B}{B_n}\right)^{0.5} \tag{3}$$

where B is the gross section thickness and

$$K = \sigma\sqrt{a}\, Y(a/W) \tag{4}$$

where *Y(a/W)* is a function of geometry, crack length *a* and width *W*.

Y(a/W) functions for stress intensity factors for various geometries are given in [7]. For specimens loaded under a tensile load *P*, the membrane stress, σ_m, is given by

$$\sigma_m = P/(BW) \tag{5}$$

(Replace *W* with 2*W* for DEN(T) and M(T) specimens), and for specimens subjected to a constant bending moment *M* the nominal bending stress at the outer fibre (surface) is given by

$$\sigma_b = 6M/(BW^2) \tag{6}$$

*6.2. Creep Crack Growth Rate Correlations Using C**

The choice of the appropriate crack growth rate correlation parameter depends mainly on the material behaviour under service conditions, whether the material exhibits creep-ductile or creep-brittle behaviour [1, 10, 16]. Steady-state creep crack growth rates in creep-ductile materials, exhibiting extensive creep, are correlated with *C**. In the small-scale creep region the parameter C_t [13] could also be used. However, for most practical examples in laboratory test pieces, it can be assumed that $C_t \cong C^*$ [2, 16]. Therefore this procedure will adopt *C** for use in the correlation of the data for extensive creep conditions.

*C** can be determined experimentally or using numerical and limit analysis methods. The latter methods are generally employed for calculating *C** values for components.

The creep crack tip characterizing parameter, *C**, defined under widespread, steady state creep conditions, is analogous to J_p for a non-linear elastic material. Hence for a power law creeping material, *C** may be determined from the load displacement rate record during a creep crack growth tests using the relation

$$C^* = \frac{P\dot{\Delta}_c}{B(W-a)} H\eta \tag{7}$$

In Eqn. (7) the values of *H* and η for a power law creep material, with creep exponent *n*, are the same as those for a power law plastic material with exponent, *N*, when it is assumed that *n=N*. Eqn. (7) is used in ASTM E1457 to derive *C** for homogenous materials. In using the same equation for weldments and inhomogeneous alloys it is assumed that instantaneous load-line displacement in each test is a measure of the overall response of the crack tip creep behaviour [17]. Hence the variability in creep properties will give an average behaviour in Displacement rate which directly affects the calculation of *C** in Eqn 7.

6.3. Determination of C from LLD and CMOD Rates*

The experimental *C** parameter for a power law material may be estimated from the creep components of load line displacement rate, $\dot{\Delta}^{LLD}$, or crack mouth opening displacement rate, $\dot{\Delta}^{CMOD}$, using Eqns. (8) and (9), respectively [13,18],

Field Code Changed

Field Code Changed

$$C^* = \frac{P\dot{\Delta}_c^{LLD}}{B(W-a)} H^{LLD}\eta^{LLD} \tag{8}$$

$$C^* = \frac{P\dot{\Delta}_c^{CMOD}}{B(W-a)} H^{CMOD} \eta^{CMOD} \tag{9}$$

where P is the applied load, W is the specimen width (or half width for DEN(T) and M(T) specimens) and B is the specimen thickness. Some of the solutions for the geometric functions H^{LLD}, H^{CMOD}, η^{LLD} and η^{CMOD} for test specimens are given in Table 2. For all geometries examined, apart from M(T), DEN(T) and SEN(B), both H^{LLD} and H^{CMOD} are equal to $n/(n+1)$. The mean values of η^{LLD} and η^{CMOD}, have been used in the analysis for all geometries. The C* values determined from experimental data using $\dot{\Delta}^{LLD}$ and $\dot{\Delta}^{CMOD}$ are correlated with crack growth rate, da/dt, for SEN(B) and SEN(T) specimens in Fig. 6. Although the difference is small, a tendency is observed for higher C^* values determined from $\dot{\Delta}^{LLD}$.

Field Code Changed

Field Code Changed

Table 2 Definitions of η^{LLD}, η^{CMOD}, H^{LLD} and H^{CMOD} for each specimen. [18]

C(T)	$H^{LLD} = H^{CMOD} = n/(n+1)$	
	$\eta^{LLD} = \eta^{CMOD} = 2.2 \pm 0.1$	$0.45 \le a/W \le 0.7$
	$\eta^{LLD} = \eta^{CMOD} = 2 + 0.522(W-a)/W$	ASTM E1457-00 [1]
CS(T)	$H^{LLD} = H^{CMOD} = n/(n+1)$	
	$\eta^{LLD} = \left(7\frac{a}{W} - 0.64\right) \pm 0.6$	$0.2 \le a/W \le 0.4$
	$\eta^{CMOD} = \left(4.6 - 1.6\frac{a}{W}\right) \pm 0.2$	$0.2 \le a/W \le 0.55$
DEN(T)	$H^{LLD} = H^{CMOD} = \frac{1}{2}(n-1)/(n+1)$	
	$\eta^{LLD} = \left(0.53\frac{a}{W} + 0.42\right) \pm 0.22$	$0.3 \le a/W \le 0.7,\ 2 \le L/W \le 4$
	$\eta^{CMOD} = \left(1.26 - 0.80\frac{a}{W}\right) \pm 0.20$	$0.1 \le a/W \le 0.5,\ 2 \le L/W \le 4$
M(T)	$H^{LLD} = H^{CMOD} = \frac{1}{2}(n-1)/(n+1)$	
	$\eta^{LLD} = 0.99 \pm 0.10$	$0.35 \le a/W \le 0.7,\ 2 \le L/W \le 4$
	$\eta^{CMOD} = \left(1.26 - 0.36\frac{a}{W}\right) \pm 0.15$	$0.1 \le a/W \le 0.7,\ 2 \le L/W \le 4$
SEN(B)	$H^{LLD} = n/(n+1)$	
	$H^{CMOD} = \frac{2L}{W} n/(n+1)$	
	$\eta^{LLD} = \left(0.56\frac{a}{W} + 1.65\right) \pm 0.07$	$0.3 \le a/W \le 0.7$
	$\eta^{CMOD} = \left(0.92 - 0.46\frac{a}{W}\right) \pm 0.06$	$0.1 \le a/W \le 0.7$
SEN(T)	$H^{LLD} = H^{CMOD} = n/(n+1)$	
	$\eta^{LLD} = \left(5.0\frac{a}{W} - 0.06\right) \pm 0.38$	$0.1 \le a/W \le 0.5,\ 1 \le L/W \le 3$
	$\eta^{CMOD} = 1.0 \pm 0.05$	$0.1 \le a/W \le 0.7,\ 1 \le L/W \le 4$

The total load line displacement rate measured during the tests, $\dot{\Delta}^{LLD}$, can be partitioned into an instantaneous part, $\dot{\Delta}_i^{LLD}$, and a time-dependent part that is directly associated with the accumulation of creep strains, $\dot{\Delta}_c^{LLD}$, such that,

$$\dot{\Delta}_c^{LLD} = \dot{\Delta}^{LLD} - \dot{\Delta}_i^{LLD} \tag{10}$$

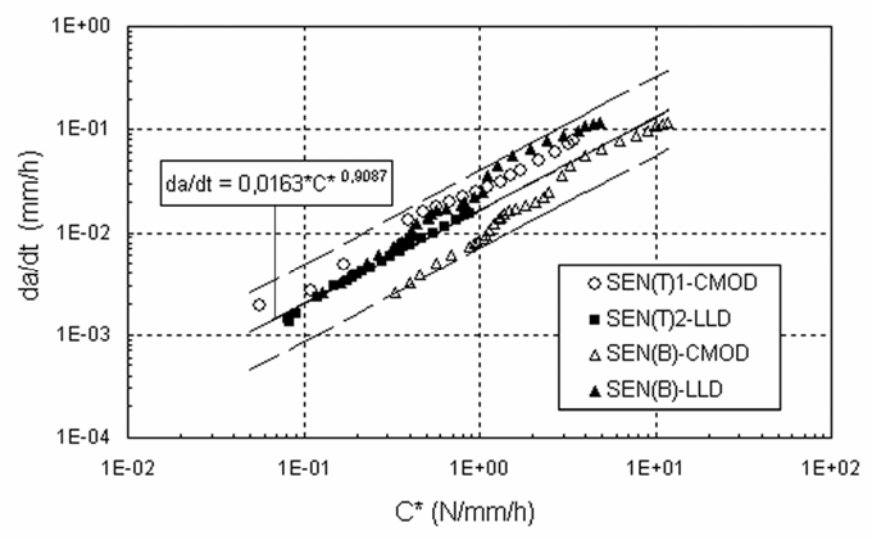

Fig. 6. CCG rate as a function of C^* calculated using Crack Mouth Opening Displacement (CMOD) and Load Line Displacement (LLD) SEN(T) and SEN(B) [19]

The instantaneous displacement rate, $\dot{\Delta}_i^{LLD}$, can be further divided into an elastic and a plastic part, with the elastic part of the instantaneous load line displacement rate, $\dot{\Delta}_{i,e}^{LLD}$, calculated as

Field Code Changed

$$\dot{\Delta}_{i,e}^{LLD} = \frac{\dot{a}B_n}{P}\left[\frac{2K^2}{E'}\right] \tag{11}$$

where $\dot{a}$ is the crack growth rate and E' is the effective elastic modulus ($E/(1 - \nu^2)$ for plane strain and E for plane stress). ASTM E 1457 [1] also provides relations for the plastic instantaneous displacement rate. Inclusion of the plastic displacement rate in Eqn. 10 is particularly important in analyses of creep ductile materials. However, it may lead to negative values of $\dot{\Delta}_c^{LLD}$ [20]. Furthermore the presence of limited plasticity will act as redistribution of crack tip stresses similar to creep and will therefore assist in CCI. Similar problems have also been encountered when using Eqn. (11) to estimate elastic displacement rates [21]. In any case, for most practical situations under creep-ductile conditions of steady state creep crack growth, the instantaneous displacement rate is insignificantly less than the total displacement rate and good correlation is found between crack growth rate and C^* evaluated using the total displacement rate, $\dot{\Delta}^{LLD}$ [19].

Field Code Changed

Field Code Changed

*6.4. Validity Criteria for the Use of C**

Validity criteria are specified in ASTM E 1457 [1] for the use of C^* as a correlating parameter for CCG data determined by testing C(T) specimens. Firstly, the transition time, t_T, must be exceeded [22]. During a test t_T is estimated from, [1],

$$t_T = \frac{K^2\left(1-\nu^2\right)}{E\left(n+1\right)C^*(t_T)} \tag{12}$$

which assumes plane strain and elastic or small-scale yielding conditions. Although not specified in ASTM E 1457 and not performed here, it has been proposed in [22] that if there is significant plasticity on loading then K^2/E in Eqn. (12) may be replaced by J.

Since the calculation of t_T depends implicitly on time through $C^*(t_T)$, its value is estimated by applying Eqn. (12), to each data point. Thus the value of t_T is given by the maximum value with time t calculated in the test data set [1,22], *i.e.*

$$t_T = \max\left[\frac{K^2\left(1-\nu^2\right)}{E\left(n+1\right)C^*(t)}\right] \tag{13}$$

In additional to satisfying the condition that $t > t_T$, if the C^* parameter is to be applied it is necessary to identify the material as 'creep-ductile' in the test regime. Data are considered to be creep-ductile if the creep load line displacement rate, calculated using Eqns. (10) and (11), constitutes at least half of the total load line displacement *i.e.* $\dot{\Delta}_c^{LLD}/\dot{\Delta}^{LLD} \geq 0.5$. For creep-brittle situations (*i.e.* $\dot{\Delta}_c^{LLD}/\dot{\Delta}^{LLD} \leq 0.25$) the stress intensity factor, K, may be used to describe the creep crack growth rate data [1] .

Finally, following ASTM E 1457 [1], the CCG rate data obtained prior to a crack extension Δa=0.2 mm are assumed to comprise a part or the whole of the crack initiation and transient region, during which the damage distribution ahead of the crack tip reaches a steady state. Therefore, these data are not included when plotting crack growth rate against C^*. However, the early stage crack growth data may be correlated with K and/or C_t or local CTOD. The loading conditions and crack tip stress-strain state need to be analyzed and reported.

7. Treatment of Creep Crack Initiation

Creep crack initiation (CCI) could constitute a major portion of the time to failure. The collected data for initiation times to a crack extension of 0.2 mm and 0.5 mm can be correlated with K, C^* [23]. Other crack tip parameters, (C_t, local CTOD and Q*) may also be used for CCI correlations. However, their use has not been verified for the present CoP. In most cases, initiation times are inversely proportional to the crack tip parameters. The experimental verification is shown in the section "Validation of CoP", below.

8. Recommended Minimum Number and Duration for Tests

When design and defect assessment calculations are based on 'enough' data, the base values should be reproducible, to within engineering accuracy, across comparable data sets. The objective of the CoP is to highlight issues associated with the small-sample reproducibility and to provide guidance on how many data are necessary in base value calculations in order for these values to be approximately reproducible. How many data are 'enough' depends on many factors, including: statistical model, anisotropy of the material,

degree of reproducibility, variability in the measured property, variability in measurements, accuracy of the equipment, and cost and the capability of performing tests.

It is recommended that tests loads are designed so that the range of CCG rate measure from one test overlap another test. In this way continuity of the slope for CCG rate can be observed. The minimum number of tests should be increased when the data from a weldment zone (e.g. cross-weld and Heat Affected Zone (HAZ) specimens) show scatter [10]. Also, more tests should be performed if the material CCG behaviour exhibits increased scatter regardless of the reason for the variability. If there is insufficient material available or if there are other reasons, which would restrict multiple testing then the results should be considered with increased caution. Because of these factors, it is impossible to give firm recommendations but a minimum number of five tests are suggested at different loads. Batch to batch variation is more important in welds and cross-weld samples than in parent metallic materials. This is due to sensitivity of the properties on fabrication processes. Background information and guidelines about fabrication and test-piece preparation to assist the tester in making a sample size decision should be planned. It should be emphasized that differences and the stability of the material base values with respect to sample size and geometry need to be taken into account.

The hold time at temperature prior to the start of a test should be governed by the time necessary to ensure that the temperature can be maintained within ±2°C [10]. This time will not be less than one hour per 25 mm of specimen thickness. The test duration may be estimated for guidance from applied load and materials data at test temperature, using K formulae for crack initiation. The calculated value will be revised after the first test for a more accurate test duration estimation. If failure of the specimen occurs prior to stopping a test then measurements of the final crack size on the fractured surface may not be possible. In this case or when $\Delta a/a_o > 0.2$ an upper bound estimate of the final crack size should be made (i.e. $< 0.75a/W$). However, a repeat test may also be needed.

9. Validation of the CoP

The validation of the CoP is based on extensive analyses of the results from European collaborative work [7,10,18,19,21]. The experimental data are analyzed and correlated with pre-determined crack tip parameters. The CCI data for two geometries is correlated with both K and C^* parameters in Figs. 7-10. Additional data obtained on RNB(T) specimens are also included in C* correlation of crack initiation times in Figs. 9 and 10. Although general tendency is seen in linear fit of data from different zones (BM, HAZ, WM) of weldments, deviation in K correlation is seen in HAZ showing reduced crack initiation resistance at longer exposure time at test temperatures. A similar effect is seen in C* correlations in BM, followed by HAZ. These observations direct attention to choice of load level and test conditions for different zones of a weld steel where deterioration of crack resistance at the crack tip is seen.

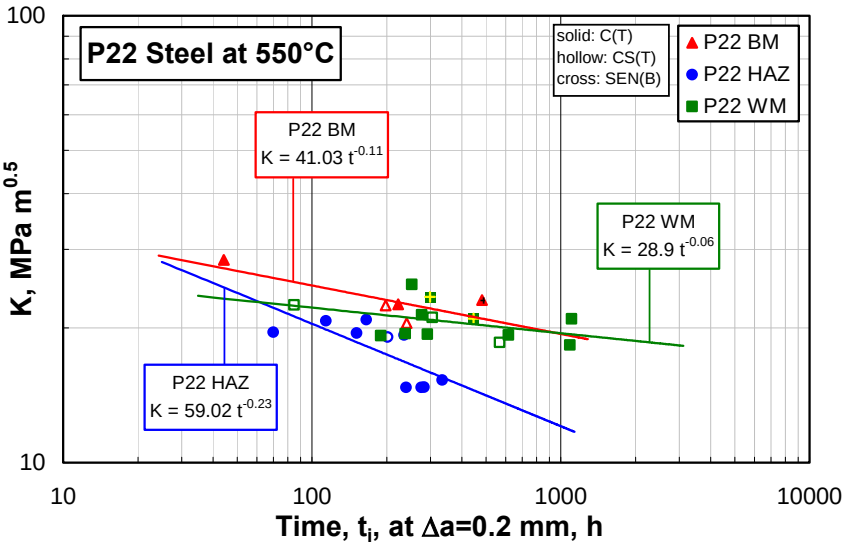

Fig. 7. *K* vs. time to crack initiation defined at crack growth Δa=0.2 mm for P22 at 550°C

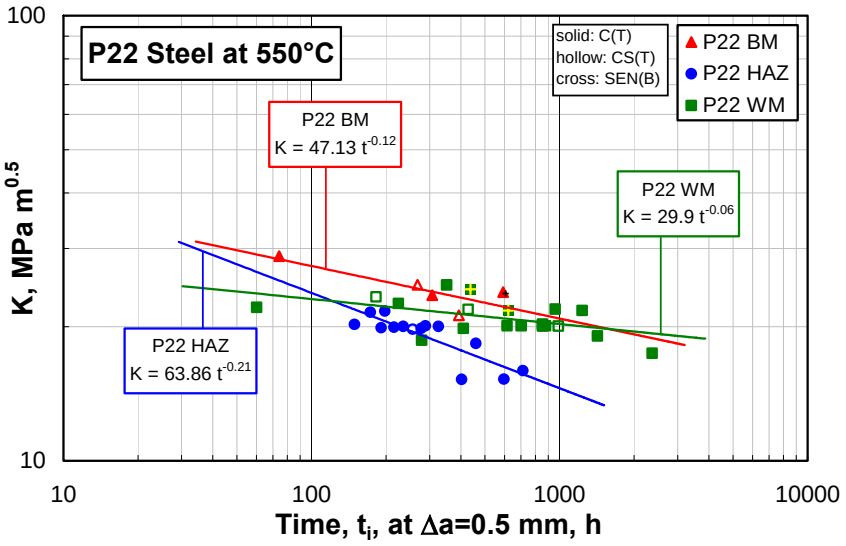

Fig. 8. *K* vs. time to crack initiation defined at crack growth Δa=0.5 mm for P22 at 550°C

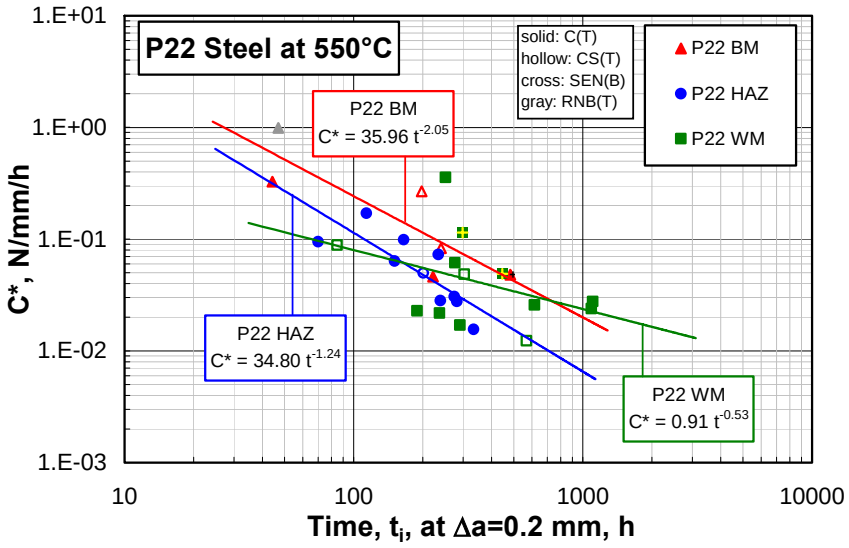

Fig. 9. C^* vs. time to crack initiation defined at crack growth Δa=0.2 mm for P22 at 550°C

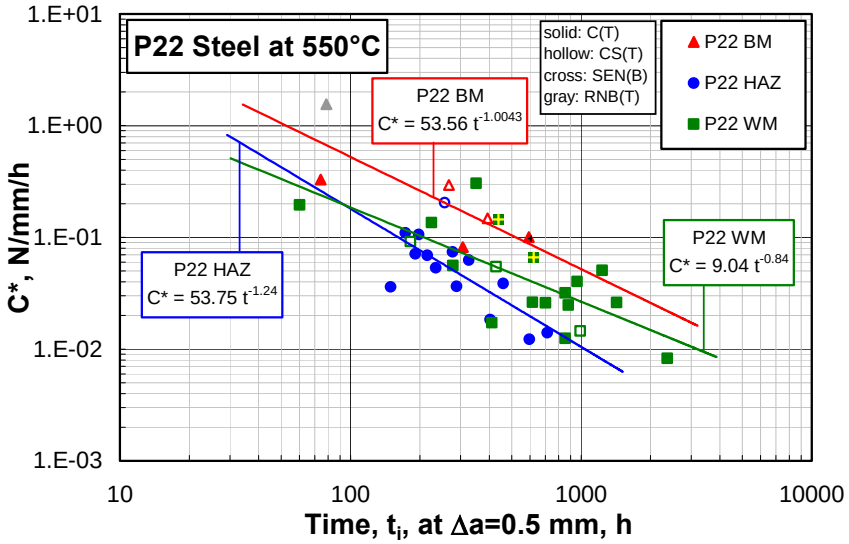

Fig. 10. C^* vs. time to crack initiation defined at crack growth Δa=0.5 mm for P22 at 550°C

The users of the CoP are advised, in any event, to correlate CCI and CCG data with K and C^* using the formulae given in [7,21] and report their findings. The same condition regarding the validity of K or C^* will apply for CCG. The CCG data obtained from tests on different geometries are presented in Figs. 11-14. The presented data demonstrate the applicability of the crack tip parameters for correlating CCG of weldments with crack tip located in different weldment zones. Figures 11-14 include all data from different laboratories, that point out lab-to-lab variation of data and its analysis, emphasizing the need for harmonization of CCG testing and assessment. Note that the data received from the partners are assessed following the present CoP. It has been found that the method of data reduction slightly affects the scatter

in the results. Generally, the figures show a high scatter in *K* correlation of CCG rate whereas much improved correlation with *C** in the valid steady state range is seen. This demonstrates the applicability of the present CoP to weldments characterisation for CCI and CCG. This is particularly important where the data are used for assessment of welded components of utilities in high temperature service.

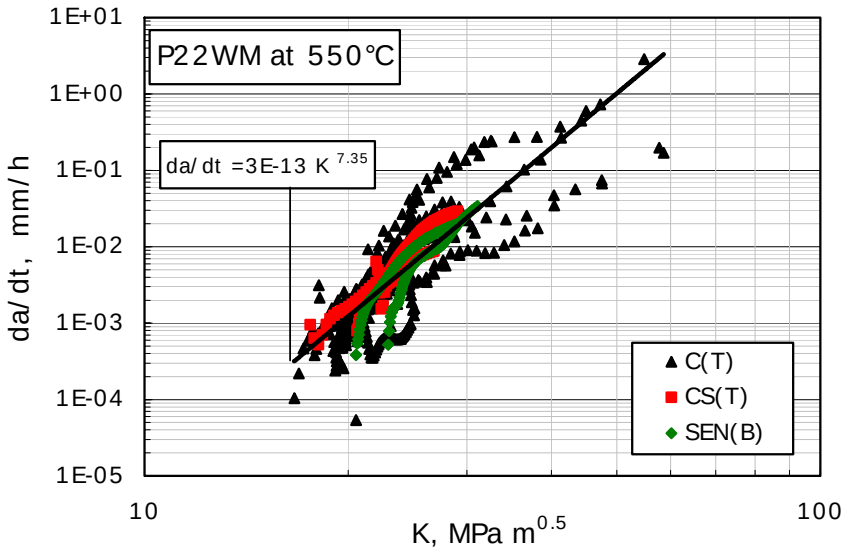

Fig. 11. Crack growth rate vs. *K* for P22 WM at 550°C

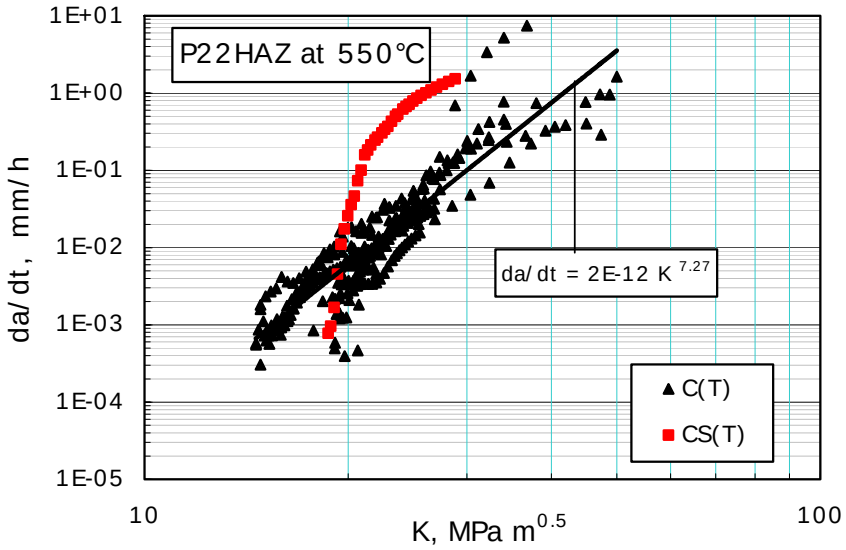

Fig. 12. Crack growth rate vs. *K* for P22 HAZ at 550°C

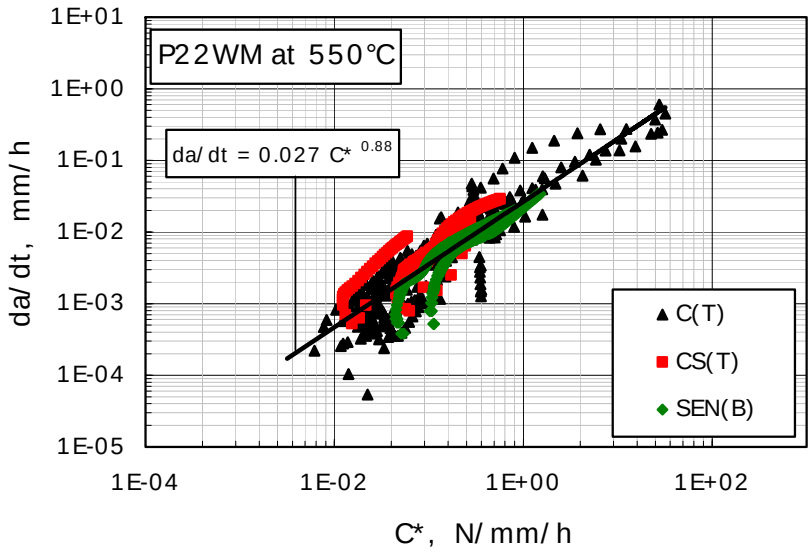

Fig. 13. CCG rate of P22 WM as a function of C^* calculated using Load Line Displacement (LLD) rates of C(T) and CS(T)

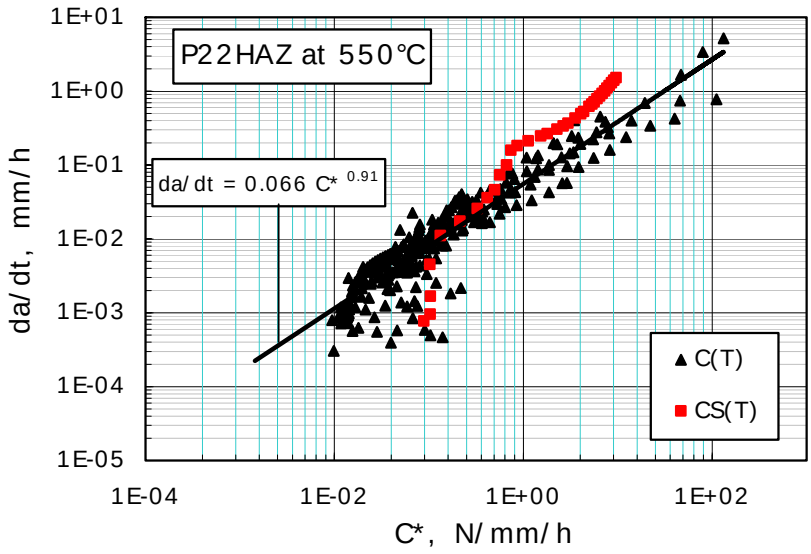

Fig. 14. Crack growth rate vs. C^* for P22 HAZ at 550°C

The crack initiation time, t_i, correlated with K gives less scatter. This may be checked with validity criteria (Eqn. 12) for K and C^* correlation. As a general observation, the CCI is seen prior to extensive creep deformation sets in, therefore, K correlation is conceivable. Geometry effect on CCI and CCG correlations is seen in RNB(T) data in particular. The C^* is a correlation parameter with less scatter than K, especially at initial and higher crack growth rates.

10. Application of Data for Assessment

The draft CoP [7] can be used to determine experimental crack initiation and crack growth rate correlations for assessment of components in high temperature service. The correlations of steady state crack initiation and growth, CCI and CCG, rate with K and C^* can be represented by straight lines of different slopes on log/log plots and expressed by power laws of the form as shown in Figures

For CCI as

$$t_i = \frac{\Delta a}{\dot{a}} = \frac{D_i^{'} \Delta a}{K^{m'}} \tag{14}$$

$$t_i = \frac{\Delta a}{\dot{a}} = \frac{D_i \Delta a}{C^{*\phi}} \tag{15}$$

And for CCG as

$$\dot{a} = D' K^{m'} \tag{16}$$

$$\dot{a} = D_o C^{*\phi} \tag{17}$$

A steady state relationship between crack growth rate and the parameters in Eqns (16) and (17) physically implies a progressively accelerating creep crack growth rate. For a conservative assessment the use of CCG data in the above equations are sufficient [24]. However, CCI predictions using Eqns. (19,20) can also be considered.

11. Discussion and Conclusions

The presented CoP provides guidelines for specimen selection, testing and data analysis for weldments that include novel aspects such as the use of new geometries for testing creep crack initiation and growth. The CoP has been validated using tests on P22, P91 similar welds and P91-316 dissimilar welds. Additional validation is provided on C-Mn and 316H steels conducted within the CRETE [2] project. The higher ductility materials require special attention to be paid to test load level and the potential for significant plastic deformation; this can result in particular difficulties in correlating initiation times with K. These problems could be overcome by correlating initiation times with the creep crack initiation toughness, K_{mat}^{c}, as this parameter explicitly incorporates the effects of elastic, plastic and creep deformation [21]. C^* correlations provide CCG rate information with minimum scatter for component assessment. The analysis using K and C^* solutions for CCI and CCG, $Y(a/W)$ and η factors for the geometries and type of loading covered by the CoP have been verified [18,19]. These results suggest that the CoP may be followed for testing and analyses for the range of geometries and dimensions. There are size and geometry effects on CCI and CCG behaviour of tested materials. The size effect may be accounted for through geometrical variable in data analysis. However, the geometry effect is obvious, particularly in RNB(T) specimen.

Field Code Changed

Machine capacity, material availability and the volume and dimensions of usable material restrict the choice of geometry in many cases. This issue is of particular concern when testing material obtained from components containing welds in both virgin and service exposed conditions. The location and orientation of the crack in the specimen also need to be consistent with the defect orientation in the component being assessed. Recommendations have been presented regarding the optimum choice of specimen geometry. Highly constrained C(T), SEN(B) and CS(T) specimens will require lower test loads for given ligament

dimensions, B_n, (W-a), than the DEN(T) and M(T) geometries. The stress state of the component and the mode of loading on the component could also influence the choice of specimen.

The creep crack growth rate value at a given C^* can vary as a result of inherent scatter in material response if all other variables such as geometry, specimen size, crack size, loading method and temperature are kept constant. This scatter may be increased further by variables such as microstructural differences as in weldments, loading precision, environmental control, and data processing techniques. Confidence in the data will increase with the number of tests performed on any one batch of material. Using reduced number of tests rather than full set of available tests to characterize the CCG behaviour of a material may yield unreliable results (Figs. 6, 13). A valid set of data for use in subsequent structural analysis should include analysis of the data together with information from metallographic examination of the test specimens.

The extent of plasticity and the level of crack tip blunting will influence the short time tests with test durations <5000h, depending on the tensile strength of the material. Therefore, it is advisable to maximize test durations as far as possible. Otherwise, when using short-term data to assess long term component life the analysis should be treated with caution. It is commonly observed that creep rupture ductility decreases with increasing test duration [25]. Intergranular cavitation increasingly dominates the failure mechanism at longer times. In crack initiation and growth tests, the multi-axial stress state ahead of a crack promotes low displacement failures. For material in weld zones that cavitate readily, such mechanisms may be reproduced by testing at higher stress levels. However, in materials where the low stress mechanism is replaced by matrix deformation dominated failure at higher stresses, it may be necessary to accelerate tests by increasing temperatures rather than stresses. In either case, it is essential that the mechanisms operative in the test specimen lead to deformation resembling the service conditions.

It should also be noted that the present work does not account for the effects of residual stresses in the weld. This will be investigated in the Versailles Agreement on Advanced Materials and Standard, Technical Working Area, VAMAS TWA31 collaboration committee that is a follow up of the work started in ESIS TC11 group.

The present CoP may be followed to produce CCI and CCG properties data for creep brittle/ductile materials including weldments. Guidelines for testing and analyses of industrially relevant specimen geometries and sizes are provided. The data will be produced with an acceptable experimental scatter which may be used for assessment of service performance of high temperature weldments.

Acknowledgements

The work leading to production of the CoP has been done in ESIS TC11, WG on high temperature testing weldments. The contribution from EC financed CRETE project partners is also gratefully acknowledged.

References

1. ASTM E 1457-00: Standard Test Method for Measurement of Creep Crack Growth Rates in Metals", Annual Book of ASTM Standards. 2001; 3(1): 936 – 950.
2. EC Project CRETE: "Development and Harmonization of Creep Crack Growth Testing for Industrial Specimens – A Root to a European Code of Practice", EC Project No: GRD2-2000-30021.
3. Dogan B. High temperature defect assessment procedures, Int Jnl of Pressure Vessels and Piping 2003; 80: 149-156.
4. Dogan B and Ainsworth R. Defect assessment procedure for low to high temperature, ASME Conference PVP2003-2032, 2003; 463:105-111.
5. British Standards Institution, Guide on methods for assessing the acceptability of flaws in

metallic structures, BS 7910: 1999; Incorporating Amendment No 1, 2000.
6. R5 Issue 3, An Assessment procedure for the high temperature response of structures, British Energy Generation Ltd. Procedure, 2003.
7. Dogan B, Nikbin K, Webster GA, Ceyhan U, Petrovski B, Dean DW Ainsworth RA, Chapuliot S and Holdsworth S. Code of Practice for High Temperature Crack Initiation and Growth Testing of Weldments, IIW Doc., Res.XI#1, Submitted to IIW SC STAND for ISO standardisation; 2005.
8. Dogan B, Schoeneich D, Schwalbe K.-H. and Wagner R. Fatigue pre-cracking and fracture toughness testing of TiAl intermetallics. Intermetallics 1996; 4: 61-69.
9. Yokobori AT Jr., Shibato, M., Tabuchi M, and Fuji A. Comparative study of the estimation of creep crack growth behaviour of TiAl by using a pre-cracked and a notch specimen. Materials at High Temperatures 1998; 15 (2): 57-62.
10. Dogan B. High Temperature Testing of Weldments. ESIS TC11, WG: on High Temperature Testing Weldments; 2001-2005.
11. ASTM E 1737-96: Standard Test Method for J-Integral Characterization of Fracture Toughness", Annual Book of ASTM Standards. 1996; 3(1): 994-1017.
12. Rinaldi C, Dogan B, Ceyhan U and Bicego V. Analysis of creep crack growth tests on specimens with different geometries made of AISI 316H and C-Mn steels. 5th International ASTM/ESIS Symposium on Fatigue and Fracture Mechanics, Reno, NV, 18-20 May 2005.
13. Saxena A. Creep Crack Growth under Nonsteady-State Conditions. Fracture Mechanics ASTM STP 905 1986; 17: 185–201.
14. Yokobori AT Jr. and Yokobori T. New Concept to Crack Growth at High temperature Creep and Creep-Fatigue. Proc.Int. Conf. ICF7, Eds. Salama, K. et al., Pergamon press, 1989; 2:1723-1735.
15. Saxena A, Dogan, B and Schwalbe K.-H. Evaluation of the Relationship between C^*,δ_5 and δ_t During Creep Crack Growth. Proc.ASTM 24th Symp. on Fracture Mechanics. ASTM-STP 1207 1994: 510-526.
16. Special Issue on Crack Growth in Creep-brittle Materials. Eng Frac Mech 1999; 62 (1).
17. Davies CM, O'Dowd NP, Dean DW, Nikbin KM and Ainsworth RA. Failure Assessment Diagram Analysis of Creep Crack Initiation in 316H Stainless Steel. Int Jnl of Pressure Vessels and Piping 2003; 80(7-8): 541-551.
18. Davies CM, Kourbetis M, O'Dowd NP and Nikbin KM. Experimental Evaluation of the J or C* Parameter for a Range of Cracked Geometries. 5th International ASTM/ESIS Symposium on Fatigue and Fracture Mechanics, Reno, NV, 18-20 May 2005.
19. Dogan B, Ceyhan U, Nikbin K, Petrovski B. and Dean DW. European Code of Practice for Creep Crack Initiation and Growth Testing of Industrially Relevant Specimens. J of ASTM International 2006; 3(2); Paper ID: JAI13223, available online at www.astm.org.
20. Fookes AJ and Smith DJ. The Influence of Plasticity in Creep Crack Growth in Steels. Int Jnl of Pressure Vessels and Piping 2003; 80(7): 453–463.
21. Dean DW and Gladwin DN. Characterization of Creep Crack Growth Behavior in Type 316H Steel Using Both C* and Creep Toughness Parameters. Proc 9th Int. Conf. on Creep and Fracture of Engineering Materials and Structures, Swansea, April 2001: 751-761.
22. Riedel H and Rice JR. Tensile Cracks in Creeping Solids, Fracture Mechanics 12th Conference 1980; ASTM STP 700: 112-130.
23. Dogan B, Petrovski B and Ceyhan U. Significance of creep crack initiation for defect assessment. Proc. of Int. Conf. BALTICA VI, Espoo, Finland, 2004, VTT Symp.234; 2: 595-607.
24. Webster GA and Ainsworth RA. High Temperature Component Life Assessment, 1st Edition. London: Chapman and Hall, 1994.
25. EU Project Advanced Creep WG1. European Creep Collaborative Committee. Coordinator: A. Shibli, European Technology Development (ETD) Ltd., EC Project No: G1RT-CT-2001-05042.